ELSEVIER

www.elsevier.nl/locate/jorganchem

Journal of Organometallic Chemistry 621 (2001) 267–276

Journal of Organometallic Chemistry

Preparation and crystal structures of the complexes $(\eta^5\text{-}C_5H_3TMS{-}CMe_2{-}\eta^5\text{-}C_{13}H_8)MCl_2$ and $[3,6\text{-di}^t\text{But}C_{13}H_6{-}SiMe_2{-}N^t\text{Bu}]MCl_2$ (M = Hf, Zr or Ti): mechanistic aspects of the catalytic formation of a isotactic–syndiotactic stereoblock-type polypropylene

Abbas Razavi [a,*], Ulf Thewalt [b]

[a] *Fina Research, Centre de Recherche du Groupe TotalFinaElf, Zone Industrielle C, B-7181 Feluy, Belgium*
[b] *Sektion für Röntgen- und Elektronenbeugung, Universität Ulm, D-89069 Ulm, Germany*

Received 28 September 2000; accepted 4 October 2000

Dedicated to Professor Henri Brünner on the occasion of his 65th birthday

Abstract

The reaction of MCl_4 (M = Zr or Hf) with the dilithium salt of 2-(3-trimethylsilyl-cyclopentadienyl)-2-fluorenylpropane in pentane leads to the formation of the complexes $(\eta^5\text{-}C_5H_3TMS{-}CMe_2{-}\eta^5\text{-}C_{13}H_8)MCl_2$ (M = Zr or Hf; TMS = trimethylsilyl). The X-ray diffraction data show that both the fluorenyl and cyclopentadienyl groups are η^5 bonded to the transition metal in these complexes in the solid phase. The polymerization data and the polymer microstructure, however, clearly indicate that at least after the activation with MAO the active species formed with these molecules show very dynamic bonding behavior and their substituted cyclopentadienyl group changes its hapticity rapidly and frequently during the course of the polymerization.

Keywords: Zirconium; Hafnium; Crystal structures; Stereospecific polymerization

1. Introduction

Metallocene dichloride structures with basic bridged cyclopentadienyl-fluorenyl ligand skeleton have attracted considerable interest in the last decade since we first reported [1] the synthesis and characterization of the original compounds $(\eta^5\text{-}C_5H_4CR_2\text{-}\eta^5\text{-}C_{13}H_8)MCl_2$ (R = Me or Ph; M = Zr or Hf) (Fig. 1 top). The structural particularities and catalytic properties of these metallocene complexes have helped to elucidate the mechanism of olefin polymerization with coordination catalysts in general and metallocene based catalysts in particular. With the help of these two compounds it was also possible for the first time to produce highly crystalline syndiotactic polypropylene with outstanding physical and mechanical properties in the laboratory and on an industrial scale. The chain migratory insertion mechanism (Fig. 1 bottom) proposed for these catalysts provides a generally accepted mechanism according to which the activated form of these prochiral, *Cs* symmetric metallocene molecules produce syndiotactic polypropylene polymer chains by alternatively incorporating the re or si faces of the propylene monomers enantio face selectively [1a,2]. Investigation of the microstructure of syndiotactic polymer produced with the Hf analog via high resolution ^{13}C-NMR revealed that the syndiotactic chains contained additionally short isotactic sequences [1,3]. It was later noted that even longer isotactic sequences can be introduced in the backbone of the syndiotactic chains if, via substitution of a single alkyl group such as methyl, isopropyl, etc. at one of the distal cyclopentadienyl positions, the *Cs* symmetry of the resulting catalysts was destroyed.

* Corresponding author. Tel.: +32-64-514072.
E-mail address: abbas.razavi@atofina.be (A. Razavi).

0022-328X/01/$ - see front matter
PII: S0022-328X(00)00863-9

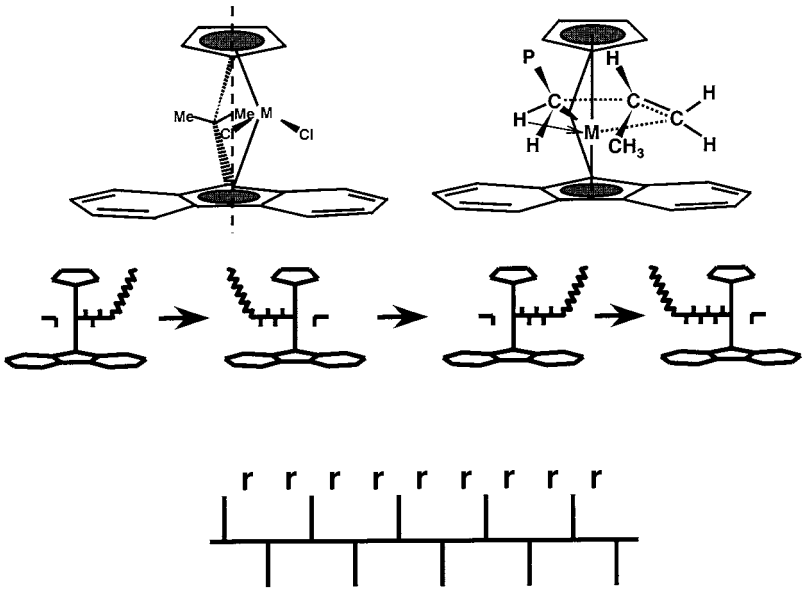

Fig. 1. Schematic representation of isopropylidene(cyclopentadienyl-fluorenyl)MCl_2 (M = Zr, Hf) (left), their transition state structures (right) and the schematic representation of entioselectitive chain migratory insertion mechanism.

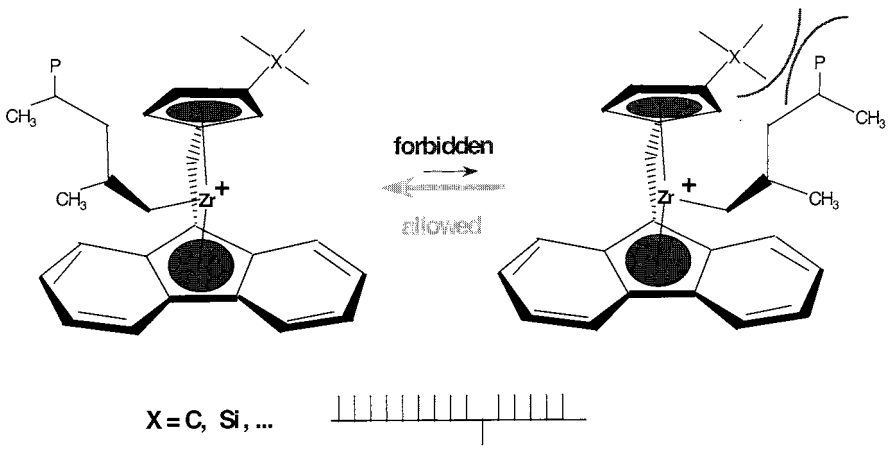

Fig. 2. Schematic representation of the chain 'stationary' insertion mechanism with a C_1 symmetric catalyst with a bulky distal substituent.

The critical size of the substituent is finally reached at the tertiary butyl group whose introduction as a substituent transforms the tactic behavior of the resulting catalyst completely.

The formation of isotactic polypropylene with the C_1 symmetric metallocene μ-isopropylidene-(3-tert-butylcyclopentadienyl-fluorenyl)zirconium dichloride (**3**) [4] was rationalized on the basis of a hindered chain migratory insertion mechanism and continuous coordination and insertion of only one of the propylene prochiral faces. This so-called chain 'stationary' insertion mechanism assumes that the steric bulk of the β-substituent hovering over one of the two diastereotopic coordination positions prevents the full migration of the growing polymer chain to that coordination site, leaving only the other coordination position available for monomer coordination (Fig. 2). The growing polymer chain would stay permanently on the less crowded position and enchain only monomers with either si or re face exclusively [4]. The Hf analog of **3**, the metallocene μ-isopropylidene-(3-tert-butylcyclopentadienyl-fluorenyl)hafnium dichloride (**4**) provides a very unstable catalyst that decomposes in solution.

In this paper we report the crystal structure and catalytic properties of a new class of bridged cyclopentadienyl-fluorenyl ligand based metallocene molecules (η^5-C_5H_3TMS–CMe_2–η^5-$C_{13}H_8$)MCl_2 (M = Zr **5**, Hf **6**) in which the selection of trimethylsilyl (TMS) as the β-substituent at the cyclopentadienyl moiety has led to new types of metallocene catalyst with bi-tactic specific behavior with respect to propylene polymerization. The mechanism proposed for the polymerization behavior

Table 1
Crystal data and refinement details for **5**–**7**

	5	**6**	**7**
Formula	$C_{24}H_{26}Cl_2SiZr$	$C_{24}H_{26}Cl_2HfSi$	$C_{27}H_{39}Cl_2NSiZr$
M_r	504.66	591.93	567.80
Crystal system	Monoclinic	Monoclinic	Orthorhombic
Space group	$P2_1/c$	$P2_1/c$	$Pcab$
Unit cell parameters			
a (Å)	10.408(3)	10.424(3)	13.372(1)
b (Å)	17.739(5)	17.706(6)	19.090(2)
c (Å)	12.147(3)	12.121(4)	22.792(3)
β (°)	93.52(3)	93.53(3)	90
V (Å^3)	2238.4(11)	2232.9(12)	5818.3(10)
Z	4	4	8
D_{calc} (g cm^{-3})	1.497	1.761	1.296
μ (mm^{-1})	0.79	4.97	0.72
Crystal size (mm^3)	$0.35\times0.20\times0.20$	$0.20\times0.20\times0.15$	$0.37\times0.18\times0.08$
T (K)	293	293	193
θ range (°)	2.75–24.5	2.75–25.0	1.79–24.1
Measured reflections	3713	4111	35697
Unique reflections	3713	3912	4445
R_{int}	Unique data set	0.031	0.196
Reflections with $I>2\sigma(I)$	2090	3166	2670
Goodness-of-fit	0.946	0.998	0.997
R_1 (F,$F^2>2\sigma$)	0.027	0.019	0.081
R_1 (F, all data)	0.076	0.030	0.120
wR_2 (F^2,$F^2>2\sigma$)	0.058	0.053	0.218
wR_2 (F^2, all data)	0.060	0.054	0.239
Minimum/maximum in ΔF (e Å^{-3})	−0.24/0.26	−0.74/0.39	−0.85/1.19

of **3** is supported by introduction of yet another class of metallocene, [3,6-di^{t}Bu$C_{13}H_6$–$SiMe_2$–N^{t}Bu]MCl_2 (M = Zr **7**, Ti **8**) which act as catalysts in a highly syndiotactic specific manner.

2. Results and discussions

The bridged ligand, 2-(trimethylsilylcyclopentadienyl)-2-(fluorenyl)propane is prepared according to a similar procedure described previously [1,3–5]. Double deprotonation of the ligand with a solution containing two equivalents of methyllithium in tetrahydrofuran (THF) leads to the formation of the corresponding dianion. The subsequent reaction of the dianion with one equivalent of MCl_4 (M = Zr, Hf) in pentane yields the red zirconium complex and yellow hafnium complex. Both complexes have been identified by their ^{1}H-NMR spectra and single-crystal X-ray structures. The identification and assignment of the signals are straightforward and were done based on the spectra of a number of similar structures reported in our previous publications [1,3–5]. The [3,6-di^{t}But$C_{13}H_6$–$SiMe_2$–N^{t}Bu]MCl_2 complexes were prepared according to similar procedures described in the literature [6]. They were characterized spectroscopically. Complex **7** was also characterized by its X-ray structure.

2.1. Molecular structures of *5* and *6*

The complexes **5** and **6** crystallize as racemates. They have almost identical cell dimensions and molecular structures. The crystal data are summarized in Table 1. The structure of **5** is illustrated in Fig. 3 and selected distances and angles are given in Table 2. As for the pair of related complexes (η^5-C_5H_4–CPh_2-η^5-$C_{13}H_8$)MCl_2 (M = Zr, Hf) [5], the Zr–Cl distances are ca. 0.02 Å longer than the Hf–Cl distances. Other differences can probably be neglected. Close similarities in cell dimensions and molecular structures between chemically analogous zirconium and hafnium complexes are common. There are, however, cases where the molecular geometries agree, whereas space groups and lattice constants are different. An example is the pair of complexes (η^5-C_5H_4–CMe_2–η^5-$C_{13}H_8$)MCl_2 (M = Zr, Hf) [1a].

Geometrical parameters for **5** and **6** are compared in Table 3 with those of related complexes. The angles α, β, γ, and ϕ (see Fig. 4) are the same as those used by Resconi et al. [7]. In the present paper δ is the angle between the normal vector of the C_5 ring and the vector connecting M with the ring center c; Resconi et al. use $90°-\delta$ instead. The data of Table 3 show that the geometrical parameters for complexes with the Cp–CR_2–flu ligand are rather uniform. The angle α (centroid–M–centroid angle) falls in the interval 117–119°

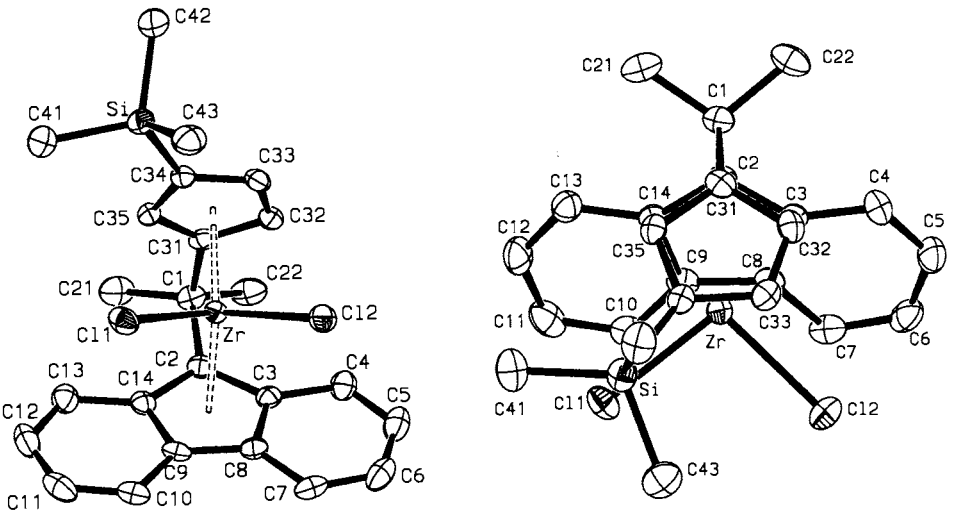

Fig. 3. Molecular structure of **5** with thermal ellipsoids at the 30% probability level; two views in parallel projection.

and β (angle between the ring planes) falls in the interval 71–74°. α for these complexes is significantly smaller than α for complexes with unbridged η^5-ligands (129.0° for Cp_2ZrCl_2 [8a] and 135.1° for $(Meflu)_2ZrCl_2$ [8c]). Replacement of a CR_2 bridge by a SiR_2 bridge also causes an increase in α (127.9° in **B** [9]). The bonding angle ϕ at the bridging C atom (98.3° in **5**, 98.9° in **6**) compares well with ϕ in related complexes containing a CR_2 bridge.

The complexes show deviations from an ideal geometry where (i) the C–C bond vector connecting the bridge with a C_5 ring would be parallel to the C_5 ring plane and (ii) a metal atom would reside exactly above the center of a C_5 ring. The deviations from this situation are measured by the angles γ and δ (see Fig. 4). In **5** and **6** as well as in other complexes with a Cp–CR_2–flu ligand γ(Cp) is somewhat larger than γ(flu) (13.7 and 11.3°, respectively, in **5**). Almost the same value for γ(Cp) as in **5** is calculated for the complex with a Cp–CMe_2–Cp ligand (14.2° in **F**) [8b].

A δ value larger than zero indicates that the metal atom is displaced from its geometrically ideal position towards the bridge. The data of Table 3 show that δ for a fluorenyl C_5 ring is considerably larger than for a Cp group in **5** and **6** and in related complexes. The data for **5** are: δ(flu) = 7.5 and δ(Cp) = 4.0°. A δ value greater than zero is accompanied by an increase of metal to ring carbon distances towards the open side of the wedge formed by the η^5 groups. The values for δ, the $M–C_{ring}$ distances and Δr, the difference between the largest and the smallest values, are surprisingly similar for the Cp fragments as well as for the Flu fragments of the ansa complexes; see Table 3. The relatively large values of δ and Δr for a fluorenyl group can be attributed to (i) repulsive non-bonded interactions between the chlorine atoms and carbon and hydrogen atoms of the fluorenyl C_6 rings [4] and (ii) an intrinsic preference of an η^5-fluorenyl ligand for an unsymmetrical arrangement of the observed type. This view is supported by the results of EHMO calculations for compounds with $C_{13}H_9^-$ and similar ligands [10]. Evidently both effects are cooperative here.

A comparison of the geometrical data for **5** and **6** with those of the parent complex **A** shows that the introduction of a TMS group at the Cp ring has little effect on the molecular structure. The Si atom of the TMS group is displaced from the Cp ring plane towards the side opposite to the metal atom by 0.21 Å for **5** and 0.25 Å for **6**. An analogous displacement of 0.31 Å for the ring-bonded C atom of a *t*-butyl group has been observed in **D** [4].

2.2. Molecular structure of 7

The molecular structure of **7** is shown in Fig. 5 and selected distances and angles are listed in Table 4. With one exception the geometrical data agree within narrow limits with the corresponding values for the analogous complex without *t*-butyl substituents in the fluorenyl unit [11]. The exception concerns the Zr–Cl distances which are longer in **7** (2.500(2) and 2.494(2) Å) than in the parent compound (2.399(1) and 2.397(1) Å [11]). The atoms Zr, N, Si and C(2) are essentially coplanar (deviating from their best plane by less than 0.02 Å). This plane and the C_5 ring plane intersect at an angle of 88.5°. As in the parent complex the nitrogen in **7** has a trigonal planar coordination. The sum of bond angles is 360.0°. The two fluorenyl-bonded C atoms of the *t*-butyl groups are essentially coplanar with the fluorenyl group atoms.

The geometry of the Zr flu fragment in **7** agrees well with that of the parent complex. The values of δ, the $Zr–C_{ring}$ distances and Δr are 7.5°, 2.38–2.64 Å, and 0.26 Å for **7** and 6.6°, 2.38–2.61 Å, and 0.28 Å for the

parent complex [11] (For the meaning of δ and Δr see Fig. 4 and the discussion of structures **5** and **6**). It should be noted that despite different overall structures of the ligand systems in **5** and **7** the geometry of the Zr flu parts in these complexes is very similar. The data for **5** are: 7.5°, 2.42–2.70 Å, and 0.28 Å. This arrangement is realized by a considerable increase of γ; 25.2° in **7** and 25.9° in the parent complex, compared to 11.3° in **5**. A value of 24.3° for γ is calculated for the structurally related complex (^{t}BuN–SiMe$_2$-η^5-C$_{13}$H$_8$)Zr-(CH$_2$SiMe$_3$)$_2$ [12].

2.3. Polymerization behavior

Complexes **5** and **6**, after activation with methylaluminoxane (MAO) or any other ionizing agents, are active catalysts for olefin polymerization. Of particular interest is their polymerization behavior with respect to propylene. Metallocene **5**, after its activation with MAO, polymerizes propylene to isotactic polypropylene at a broad range of polymerization temperatures. The polymerization conditions, results and general polymer properties are given in Table 5. Analysis of the ^{13}C-NMR spectra of the polymers prepared at different polymerization temperatures reveals that the polymer chains are composed of predominantly isotactic sequences joined by short syndiotactic blocks [13]. At 40°C the catalyst produces an isotactic polymer which contains 1.14% syndiotactic fractions (rrrr = 1.14%); by increasing the polymerization temperature to 60°C the catalyst activity increases more than threefold and the percentage of the syndiotactic fraction in the polymer increases to the level of rrrr = 1.65%. At 80°C the catalyst starts to decompose (activity drop!) and the percentage of rrrr in the resulting polymer drops below 1%. The Hf analog **6** was too unstable in solution as a cation and decomposed rapidly before producing any reasonable quantities of polymer. However, the isotactic polymer it produces during its short lifetime contains more than 3% of a syndiotactic fraction (rrrr = 3.5%).

Table 2
Selected distances (Å) and angles (°) for **5** and **6** [a]

	5 (M = Zr)	**6** (M = Hf)
M–Cl(1)	2.417(1)	2.393(1)
M–Cl(2)	2.424(1)	2.400(1)
M–cFlu	2.261(4)	2.250(4)
M–C(2)	2.422(3)	2.412(3)
M–C(3)	2.521(3)	2.518(3)
M–C(8)	2.675(3)	2.661(3)
M–C(9)	2.679(3)	2.669(3)
M–C(14)	2.548(3)	2.538(3)
M–cCp	2.176(4)	2.159(4)
M–C(31)	2.425(3)	2.424(3)
M–C(32)	2.460(3)	2.454(3)
M–C(33)	2.541(3)	2.526(3)
M–C(34)	2.553(3)	2.532(4)
M–C(35)	2.441(3)	2.421(3)
C(1)–C(2)	1.550(4)	1.546(4)
C(1)–C(21)	1.530(4)	1.542(5)
C(1)–C(22)	1.531(4)	1.528(5)
C(1)–C(31)	1.524(4)	1.525(5)
C(2)–C(3)	1.445(4)	1.455(5)
C(3)–C(8)	1.434(4)	1.426(5)
C(8)–C(9)	1.423(4)	1.444(5)
C(9)–C(14)	1.434(4)	1.422(5)
C(14)–C(2)	1.457(4)	1.449(5)
C(31)–C(32)	1.419(4)	1.420(5)
C(32)–C(33)	1.398(4)	1.404(5)
C(33)–C(34)	1.394(4)	1.401(5)
C(34)–C(35)	1.435(4)	1.436(5)
C(35)–C(31)	1.408(4)	1.413(5)
C(34)–Si	1.878(3)	1.869(4)
Cl(1)–M–Cl(2)	98.22(4)	97.31(4)
cFlu–M–cCp	118.0(2)	118.7(2)
C(2)–C(1)–C(31)	98.3(3)	98.9(3)
C(21)–C(1)–C(22)	106.6(3)	106.3(3)
C(3)–C(2)–C(14)	106.1(3)	105.9(3)
C(32)–C(31)–C(35)	105.7(3)	105.1(3)

[a] cCp = cyclopentadienyl centroid; cFlu = fluorenyl C$_5$ ring centroid.

2.4. Mechanistic aspects of the polymerization and the impact of trimethylsilyl substituents on the dynamic behavior of the catalyst; chain stationary insertion, hapticity and fluxionality [13–15]

The formation of isotactic polypropylene with a metallocene having a bulky group (tert-butyl, or trimethylsilyl) is visualized in Fig. 2. Because of the steric interaction between the large substituent and the growing polymer chain its migration to the crowded position is hindered or completely blocked. The chain becomes either 'stationary'[1] and remains at the less crowded positions or it migrates to an intermediate position and returns to its initial position immediately after each insertion [4,16,17,18f]. This results in the formation of isotactic parts of the polymer chain. Nevertheless, there exists a certain probability that occasionally, the chain manages to move to the energetically less favorable position (the probability is low but not zero) and comes into a very strong non-bonded steric interaction with the β-substituent. Under these conditions, to avoid this strong steric interaction, the chain can change its conformation by rotating towards the fluorenyl group where it comes in non-bonded contact

[1] From the perspective of the incoming monomers the chain is 'seen' to be always at the same position. This is why we prefer to call this mechanism a chain stationary mechanism for catalysts with large distal substituents and two energetically non-equivalent diastereotopic positions, to differentiate it from the site epimerization mechanism occurring in unsubstituted *Cs* symmetric systems with energetically equivalent enantiotopic positions.

Table 3
Geometrical parameters (° or Å) for **5** and **6** and related ansa zirconium complexes; see Fig. 4 for meaning of angles [a]

	Formula	ϕ	α	β	γ	δ	r(M–C_{ring}); Δr	Reference
5	$(C_5H_3TMS–CMe_2–C_{13}H_8)ZrCl_2$	98.3	118.0	73.5	Cp: 13.7	4.0	2.43–2.55; 0.12	This work
					Flu: 11.3	7.5	2.42–2.70; 0.28	
6	$(C_5H_3TMS–CMe_2–C_{13}H_8)HfCl_2$	98.9	118.7	72.1	Cp: 15.2	3.6	2.42–2.53; 0.11	This work
					Flu: 11.7	7.4	2.41–2.67; 0.26	
A	$(C_5H_4–CMe_2–C_{13}H_8)ZrCl_2$	99.4	118.6	72.0	Cp: 16.3	3.3	2.44–2.53; 0.09	[1a]
					Flu: 11.3	7.2	2.40–2.66; 0.26	
B	$(C_5H_4–SiMe_2–C_{13}H_8)ZrCl_2$	93.4	127.9		Cp:		2.46–2.53; 0.07	[9]
					Flu:		2.43–2.74; 0.31	
C	$(C_5H_4–CPh_2–C_{13}H_8)ZrCl_2$	99.1	117.6	72.8	Cp: 16.3	2.7	2.45–2.52; 0.07	[5]
					Flu: 10.0	7.6	2.42–2.68; 0.26	
D	$(t\text{-}BuC_5H_3–CMe_2–C_{13}H_8)ZrCl_2$	99.4	118.4	74.0	Cp: 13.3	5.5	2.43–2.62; 0.19	[4]
					Flu: 12.1	7.3	2.41–2.68; 0.27	
E	$[(C_5H_4–CMe_2–C_{13}H_8)ZrMe(PMe_3)]^+[B(C_6F_5)_4]^-$	98.4	119.1	71.1	Cp: 15.5	3.4	2.43–2.55; 0.12	[1b]
					Flu: 11.8	7.1	2.38–2.64; 0.26	
F	$(C_5H_4–CMe_2–C_5H_4)ZrCl_2$	99.8	116.6	71.4	14.2	4.0	2.45–2.56; 0.12	[8b]

[a] Angles not given in the original papers were calculated using the published cell parameters and atomic coordinates.

with the six-membered ring moiety of the fluorenyl. Sandwiched between two substituents the chain forces the catalytic species to change its hapticity temporarily or decompose. By changing the hapticity from η^5 to η^3 and eventually to η^1 in a reversible way (Fig. 6), however, it permits the chain to become progressively mobile intermittently and to shuttle freely between the two lateral pseudo-enantiotopic coordination positions back and forth after each insertion and to produce syndiotactic sequences. In extreme situations the cyclopentadienyl could even be detached and reattached, explaining in some cases partial and in some cases total decomposition of the corresponding catalyst at higher temperatures (metallocenes **4** and **6**).

There is no direct way to prove that the proposed reversible hapticity change is actually operative for the cases discussed above. What could be verified, however, is whether, in the case where such phenomena are involved, the resulting η^5,η^1 bonded ligand can provide the syndioselective environment to the site responsible for the formation of syndiotactic sequences. Thus instead of the impossible task of finding spectroscopic evidence for the occurrence of haptotropy, we took the indirect experimentally feasible approach to verify the syndiotactic selective nature of *Cs* symmetric catalysts with a η^1,η^5 bonded ligand system in which the cyclopentadienyl moiety is replaced by a single atom, e.g. a nitrogen. The eventual syndiotactic specific behavior of such a half-sandwich metallocene molecule would imply that the presence of the cyclopentadienyl ring as a whole is not really a necessity for syndiospecificity and would justify the proposed trihapto and/or monohapto mechanism. The bridge-head carbon atom of the cyclopentadienyl should, like any other single atom (linked to the fluorenyl part by a bridge) coordinated to the transition metal, maintain the required stereo-rigidity and guarantee the symmetry prerequisites (prochiral and bilateral). Fig. 7 shows the front view of such a molecule compared with the parent syndiospecific metallocene **1** and the putative monohapto bonded trimethylsilyl substituted system.

The molecule shown in the middle of Fig. 7 is a half-sandwich zirconocene and contains an unsubstituted fluorenyl. It produces oligomeric chains containing less than 50 monomer units and cannot be considered as a polymerization catalyst [18a,b,c]. However, if the fluorenyl in this complex is replaced with a substituted fluorenyl, e.g. the 2,7-di-tertiarybutylfluorene [18d–f] or better 3,6-ditertiarybutylfluorene and the Zr is replaced with Ti as transition metal, one obtains highly efficient stereoselective catalyst precursors. The half-sandwich metallocene, [3,6-di^{t}Bu$C_{13}H_6$–$SiMe_2$–N^{t}Bu]$TiCl_2$ (**8**) can be prepared in rather good yields. Once activated, **8** produces high molecular weight syndiotactic polypropylene polymers with very high activities. The corresponding zirconocene **7** is like its unsubstituted counterpart an oligomerization catalyst. Its X-ray structure provided the structural elucidation. The polymerization conditions and polymer analyses of **7** and **8** are given in Tables 6 and 7.

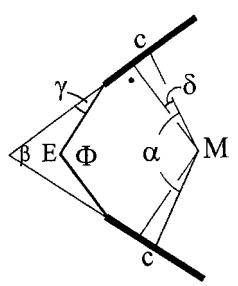

Fig. 4. Sketch indicating the angles used to describe the geometry of the bridging ligands.

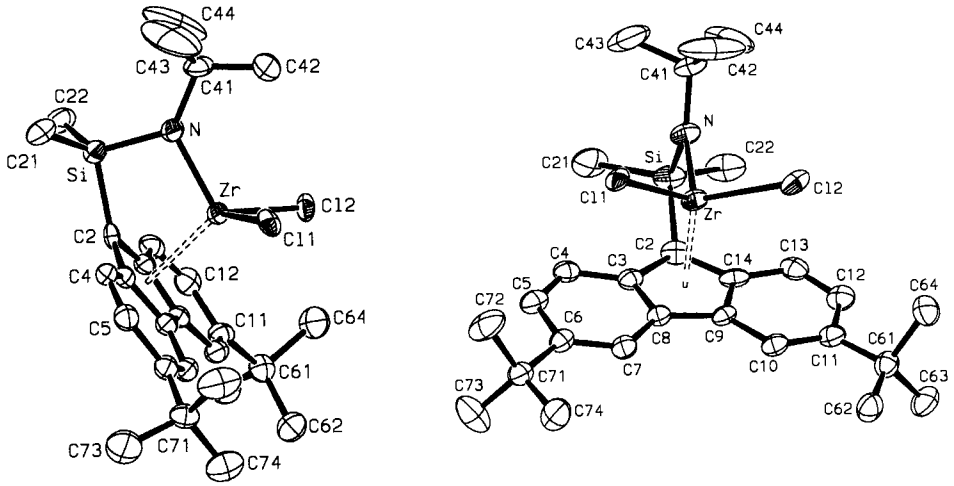

Fig. 5. Molecular structure of **7** with thermal ellipsoids at the 30% probability level; two views in parallel projection.

The microstructure of the polymer made with **8** is very similar to the microstructure of the polymers produced with the parent syndiospecific metallocenes **1** and **2** and syndiotactic stretches produced with **5**. From these results it can be deduced that a fluorenyl based η^1,η^5 bound ligand is perfectly capable of imparting the stereorigidity and symmetry environment prerequisite for syndiospecificity of the site and in this respect the proposed mechanism for **7** is justifiable. Additionally, the ^{13}C-NMR data and microstructural similarity between the syndiotactic polymer produced with **1**, (**2**), **5** indicate clearly that the formation of the polymer with **8** proceeds according to the chain migratory insertion mechanism operating on an enantiomorphic *Cs*-symmetric site (Fig. 1). The lower stereoregularity (higher heterotactic pentad fractions) of the new syndiotactic chains is probably the result of lower stereorigidity of **8** due to the dynamic environment of the nitrogen atom and/or a possible ring slippage [11,18ef] bond rearrangement mechanism leading occasionally to the asymmetry of the site and short heterotactic sequences. The higher stereoselectivity of the catalyst produced with **8** compared to very similar metallocene catalysts prepared with the 2,7-ditertiarybutylfluorene reported previously [18d–f] emphasizes the importance of the positions 3 and 6 of the fluorene part of the ligand for proper regulation of the coordinating monomer and growing polymer chain. The positions 2 and 7 are too far away from the immediate neighborhood of the active site to exert any sterically appreciable regulating effect.

3. Experimental

All operations were performed routinely under an inert gas using glove box or Schlenk techniques. Pentane and methylene chloride were dried over calcium hydride. Toluene and THF were dried over sodium benzophenone. All solvents were freshly prepared before use.

3.1. Preparation of *5*

To a suspension of 0.0175 mol of the dianion of 2(trimethylsilylcyclopentadienyl) - 2 - (fluorenyl)propane in 200 ml of dry pentane in a 1 l round bottom flask equipped with a magnetic stirring bar was added a suspension of 0.0175 mol of $ZrCl_4$ in 200 ml of pentane. The mixture was stirred for 6 h. The pentane was decanted, and the remaining red solid was extracted with methylene chloride. Cooling of the extract to -20°C gave analytically pure red crystals in 45% yield.

Table 4
Selected distances (Å) and angles (°) for **7** [a]

Zr–Cl(1)	2.500(2)	Cl(1)–Zr–Cl(2)	104.36(7)
Zr–Cl(2)	2.494(2)	N–Zr–cFlu	104.7(3)
Zr–cFlu	2.211(9)	Zr–N–Si	103.5(4)
Zr–C(2)	2.377(7)	Zr–N–C(41)	128.2(6)
Zr–C(3)	2.496(8)	Si–N–C(41)	128.3(6)
Zr–C(8)	2.636(8)	C(2)–Si–N	94.5(3)
Zr–C(9)	2.638(8)	C(21)–Si–C(22)	107.1(6)
Zr–C(14)	2.492(8)	C(3)–C(2)–C(14)	104.9(8)
Zr–N	2.040(8)		
Si–C(2)	1.854(10)		
Si–N	1.753(7)		
N–C(41)	1.493(12)		
C(2)–C(3)	1.45(1)		
C(2)–C(14)	1.46(1)		
C(3)–C(8)	1.42(1)		
C(8)–C(9)	1.46(1)		
C(9)–C(14)	1.43(1)		

[a] cFlu = fluorenyl C_5 ring centroid.

Table 5
Polymerization conditions and polymer analyses for the **5**/MAO catalyst system [a]

Catalyst (mg)	Polymerization temperature (°C)	Act. (kg/g)	MW × 10^3	M.p. (°C)	mmmm (%)	rrrr (%)
2	40	4.2	134	105.4	66.6	1.14
2	60	14.5	64	109.0	67.0	1.65
2	80	4.7	42	114.6	69.1	0.94

[a] Polymerizations were performed in a pressure reactor in 1 l liquid propylene with 5 ml of a 11 wt.% solution of MAO in toluene.

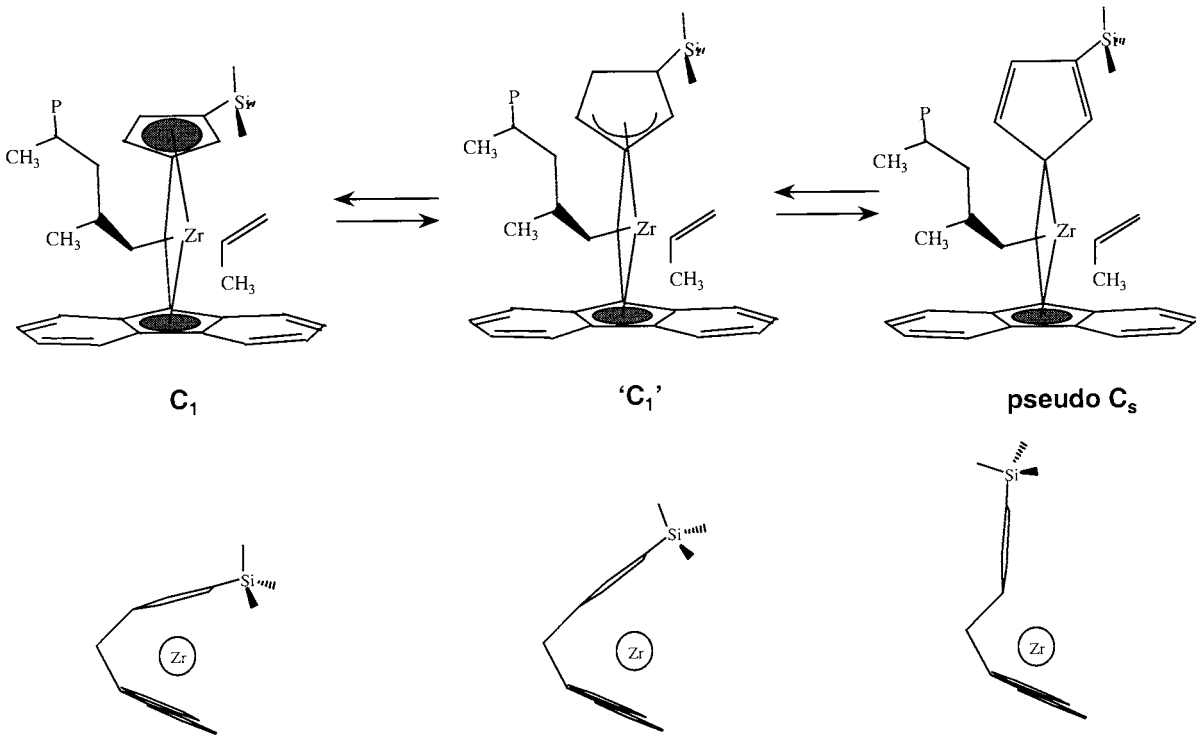

Fig. 6. Schematic representaion of hapticity change and deblockage of the crowded coordination site.

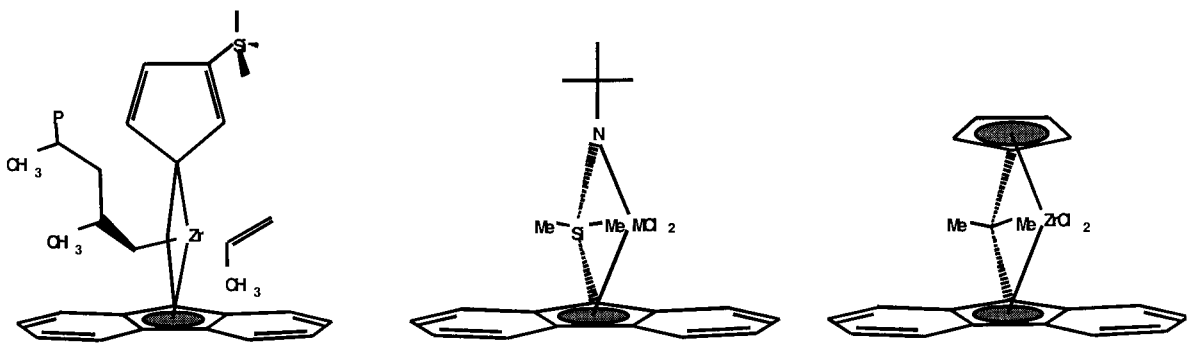

Fig. 7. Structural comparision of three syndiotactic specific catalyst precursors.

3.2. Preparation of **6**

A similar procedure to that used for the preparation of **5** was used with the difference that in this case $HfCl_4$ was employed. Consequently a yellow analytically pure product was produced (23% yield) after recrystallization of raw product from methylene chloride.

3.3. Preparation of η^1,η^5-tert-butyl-(3,6-bis-tert-butylfluorenyl-dimethylsilyl)amidodichlorozirconium (7)

3.3.1. Preparation of dimethylsilyl-(tertiarybutyl-amino)-(3,6-ditertiarybutylfluorene)

Step A. In a round bottom flask equipped with magnetic stirring bar and N_2 inlet was placed 300 ml of

diethylether (at 0°C) containing 20 g (71.8 mmol) of 3,6-ditertiarybutylfluorene. 44.9 ml of a solution containing 71.8 mmol of methyllithium in diethylether was added dropwise. The reaction mixture was stirred at ambient temperature for 4 h. The reaction mixture obtained was added dropwise to a solution of 9.27 g (71.8 mmol) of dimethyldichlorosilane in 300 ml of diethylether (at 0°C) contained in a second flask. The yellow reaction mixture was stirred at ambient temperature for 24 h.

Step B. In a round bottom flask equipped with magnetic stirring bar and N_2 inlet was placed 300 ml of diethylether (at −78°C) containing 7.6 ml (71.8 mmol) of tertiarybutylamine. Finally 44.9 ml of a solution containing 71.8 mmol of methyllithium in diethylether was added dropwise and the resulting white reaction mixture was stirred at ambient temperature for 1 h.

Step C. The product obtained in step A was added dropwise to the round bottom flask containing the reaction product of step B. The orange reaction mixture was stirred at ambient temperature for 24 h. The solid product was filtered off the solvents under N_2 and the filtrate evaporated under vacuum. After recrystallization of the residue in pentane, 22.5 g (76.84%) of an orange powder was obtained.

3.4. Preparation of η^1,η^5-tert-butyl-(3,6-bis-tert-butylfluorenyl-dimethylsilyl)amidodichlorozirconium

5 g (12.3 mmol) of tertiarybutylamin-dimethylsilylfluorene was placed in a 500 ml flask and dissolved in 250 ml of diethyl ether and cooled down to 0°C. To this solution was added dropwise 15.3 ml (24.5 mmol) of methyllithium in ether. The reaction was completed after a few hours. Evaporation of the solvent leads to the isolation of an orange powder. This powder was washed rapidly with pentane at −10°C. After filtration the product was placed in a flask containing 200 ml of pentane. 2.8578 g (12.3 mmol) of $ZrCl_4$ was added and the resulting orange reaction mixture stirred at ambient temperature for 24 h. The product was filtered. The filtrate containing the metallocene was concentrated and cooled to −10°C giving rise to orange crystals.

3.5. Preparation of η^1,η^5-tert-butyl-(3,6-bis-tert-butylfluorenyl-dimethylsilyl)amid-dichlorotitanium (**8**)

The same procedure as for the preparation of **7** was applied except in the final step $TiCl_4$ was used.

3.6. X-ray data collection, solution and refinement for **5**, **6**, and **7**

The crystals used in this study were mounted onto the end of an open Lindemann glass capillary in an oil drop. X-ray data for **5** and **6** were collected at room temperature on a Phillips PW1100 four-circle instrument and at −100°C for **7** on a STOE IPDS unit (Imaging Plate Diffraction System). Graphite monochromatized Mo–K_α radiation ($\lambda = 0.71073$ Å) was used in all cases. Crystal data are listed in Table 1 together with refinement details. The structures were solved by the Patterson method with the SHELXS-86 program [19]. The non-hydrogen atoms were refined with anisotropic thermal parameters. The structures were refined on F^2 using the SHELXL-97 program [20]. Hydrogen atoms were included in the final refinement

Table 6
Polymerization conditions and polymer analyses for the **8**/MAO catalyst system [a]

Catalyst (mg)	Polymerization temperature (°C)	Act. (kg/g)	MW × 10^3	M.p. (°C)	rrrr (%)	rr (%)
0.28	40	222	703	123.4	81.6	90.3
0.55	60	371	351	105.1	75.8	86.2
0.20	70	160		98.2	69.4	83.6
0.31	80	226	241	No peak	60.1	76.8

[a] Polymerizations were performed in a pressure reactor in 2 l liquid propylene with 4 ml of a 30 wt.% solution of MAO in toluene.

Table 7
Polymerization conditions and polymer analyses for the **7**/MAO catalyst system [a]

Catalyst (mg)	Polymerization temperature (°C)	Act. (kg/g)	MW × 10^3	M.p. (°C)	rrrr [b] (%)	rr (%)
5.13	40	16	11	151.2	86.7	94.5
5.00	60	28	6	144.9	85.7	93.7
4.86	80	63	5	140.0	83.1	93.4

[a] Polymerizations were performed in a pressure reactor in 2 l liquid propylene with 4 ml of a 30 wt.% solution of MAO in toluene.
[b] For explanation of rrrr and mmmm see Ref. [1].

cycles in a riding mode. The methyl H atoms at C(42), C(43) and C(44) in **7** were omitted, however, because of the high thermal motion of their C atoms.

4. Supplementary material

Crystallographic data have been deposited with the Cambridge Crystallographic Data Centre, CCDC Nos 147999, 147998, and 148000 for **5**, **6**, and **7**, respectively. Copies of the data may be obtained free of charge from The Director, CCDC, 12 Union Road, Cambridge CB2 1EX, UK (Fax: +44-1223-336033; e-mail: deposit@ccdc.cam.ac.uk or www: http://www.ccdc.cam.ac.uk).

References

[1] (a) A. Razavi, J. Ferrara, J. Organomet. Chem. 435 (1992) 299. (b) A. Razavi, U. Thewalt, J. Organomet. Chem. 445 (1993) 111. (c) J.A. Ewen, L.R. Jones, A. Razavi, J. Am. Chem. Soc. 110 (1988) 6256.
[2] (a) L. Cavallo, G. Guerra, M. Catatello, P. Corradini, Macromolecules 24 (1991) 1784. (b) T.A. Herzog, W.L. Zubris, J.E. Bercaw, J. Am. Chem. Soc. 118 (1996) 11988.
[3] A. Razavi, L. Peters, L. Nafpliotis, J. Mol. Catal. A 115 (1997) 129.
[4] A. Razavi, J.L. Atwood, J. Organomet. Chem. 520 (1996) 115.
[5] A. Razavi, J.L. Atwood, J. Organomet. Chem. 459 (1993) 117.
[6] (a) P.J. Shapiro, E. Bunel, W.P. Schaefer, J.E. Bercaw, Organometallics 9 (1990) 867. (b) P.J. Shapiro, W.D. Cotter, W.P. Schaefer, J.A. Labinger, J.E. Bercaw, J. Am. Chem. Soc. 116 (1994) 4623. (c) J. Okuda, J. Chem. Ber. 123 (1990) 1649. (d) J. Okuda, F.J. Schatterman, S. Wocadlo, S. Massa, Organometallics 14 (1995) 789. (e) H. Hagihara, T. Shiono, T. Ikeda, Macromolecules 31 (1998) 3184.
[7] L. Resconi, F. Piemontesi, I. Camurati, O. Sudmeijer, I.E. Nifant'ev, P.V. Ivchenko, L.G. Kuz'mina, J. Am. Chem. Soc. 120 (1998) 2308.
[8] (a) K. Prout, T.S. Cameron, R.A. Forder, S.R. Critchley, B. Denton, G.V. Rees, Acta Crystallogr. Sect. B 30 (1974) 2290. (b) R.M. Shaltout, J.Y. Corey, N.P. Rath, J. Organomet. Chem. 503 (1995) 205. (c) A. Razavi, J.L. Atwood, J. Am. Chem. Soc. 115 (1993) 7529.
[9] K. Patsidis, H.G. Alt, W. Milius, S.J. Palackal, J. Organomet. Chem. 509 (1996) 63.
[10] A. Decken, J.F. Britten, M.J. McGlinchey, J. Am. Chem. Soc. 115 (1993) 7275.
[11] H.G. Alt, K. Föttinger, W. Milius, J. Organomet. Chem. 572 (1999) 21.
[12] J. Okuda, F.J. Schattenmann, S. Wocadlo, W. Massa, Organometallics 14 (1995) 789.
[13] (a) F. Basolo, Isr. J. Chem. 27 (1986) 233. (b) A.N. Nesmeyanov, N.A. Ustynyuk, L.G. Makraova, V.G. Andrinov, Y.T. Struchkov, S. Andrae, J. Organomet. Chem. 159 (1978) 199. (c) G. Huttner, H.H. Brintzinger, L.G. Bell, J. Organomet. Chem. 145 (1978) 329.
[14] J.W. Faller, R.H. Crabtree, A. Habib, Organometallics 4 (1985) 929.
[15] F. Wild, L. Zsolnai, G. Huttner, H.H. Brintzinger, J. Organomet. Chem. 232 (1982) 233.
[16] A. Razavi, L. Peters, L. Nafpliotis, D. Vereecke, K. Den Daw, Makromol. Symp. 89 (1995) 345.
[17] A. Razavi, D. Vereecke, L. Peters, K. Den Daw, L. Nafpliotis, J.L Atwood, Mechanisms and models in Ziegler-Natta catalysis. In: R. Muelhaupt, G. Fink, H.H. Brintzinger (Eds), Int. Symp. 40 Years Ziegler Catalysts, Freiburg,, Springer, 1993.
[18] (a) H.W. Turner, G.G. Hlatky, J.A.M. Canich, WO 93/19103, 1993. (b) T. Shiomura, T. Asanuma, N. Inoue, Macromol. Rapid Commun. 17 (1996) 9. (c) H. Hagihara, T. Shiono, T. Ikeda, Macromolecules 30 (1997) 4783. (d) A. Razavi, Eur. Pat. Appl. EP0818475A1, 1996. (e) A. Razavi, D. Baekelmans, V. Bellia, Y. Debrwer, K. Hortman, M. Lambrecht, O. Miserque, M. Slawinski, L. Peters, S. Van Belle, in: T. Sano, T. Uozumi, H. Nakatani, M. Terano (Eds), Progress and Development of Catalytic Olefin Polymerization, Technology and Education Publishers, Tokyo, 2000, p. 176. (f) A. Razavi, D. Baekelmans, V. Bellia. Y. Debrwer, K. Hortman, M. Lambrecht, O. Miserque, M. Slawinski, L. Peters, S. Van Belle, in: W. Kamisky (Ed), Metalorganic Catalysts for Synthesis and Polymerization, Springer, Berlin, 1999.
[19] G.M. Sheldrick, SHELXS-86, Program for the Solution of Crystal Structures, Göttingen, 1986.
[20] G.M. Sheldrick, SHELXL-97, Program for the Refinement of Crystal Structures, Göttingen, 1997.